Provided for non-commercial research and education use.
Not for reproduction, distribution or commercial use.

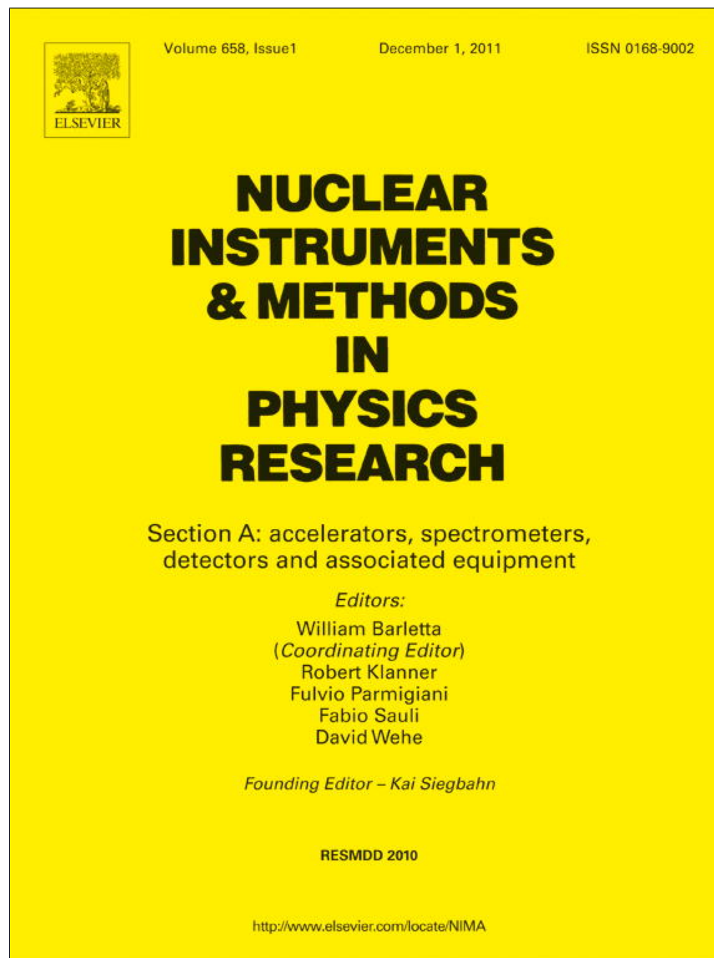

This article appeared in a journal published by Elsevier. The attached copy is furnished to the author for internal non-commercial research and education use, including for instruction at the authors institution and sharing with colleagues.

Other uses, including reproduction and distribution, or selling or licensing copies, or posting to personal, institutional or third party websites are prohibited.

In most cases authors are permitted to post their version of the article (e.g. in Word or Tex form) to their personal website or institutional repository. Authors requiring further information regarding Elsevier's archiving and manuscript policies are encouraged to visit:

http://www.elsevier.com/copyright

Author's personal copy

Nuclear Instruments and Methods in Physics Research A 658 (2011) 46–50

Contents lists available at ScienceDirect

Nuclear Instruments and Methods in Physics Research A

journal homepage: www.elsevier.com/locate/nima

Punch-through protection of SSDs in beam accidents

H.F.-W. Sadrozinski [a], C. Betancourt [a,*], A. Bielecki [a], Z. Butko [a], V. Fadeyev [a], C. Parker [a], N. Ptak [a], J. Wright [a], Y. Unno [b], S. Terada [b], Y. Ikegami [b], T. Kohriki [b], S. Mitsui [b], K. Hara [c], N. Hamasaki [c], Y. Takahashi [c], A. Chilingarov [d], H. Fox [d]

[a] *Santa Cruz Institute for Particle Physics, University of California, Santa Cruz, CA 95064, USA*
[b] *Institute of Particle and Nuclear Study, KEK, Oho 1-1, Tsukuba, Ibaraki 305-0801, Japan*
[c] *University of Tsukuba, School of Pure and Applied Sciences, Tsukuba, Ibaraki 305-9751, Japan*
[d] *Physics Department, Lancaster University, Lancaster LA1 4YB, United Kingdom*

ARTICLE INFO

Available online 1 July 2011

Keywords:
Silicon strip detectors
Punch-through protection
p-type
Laser pulses

ABSTRACT

We have tested the effectiveness of punch-through protection (PTP) structures on n-on-p AC-coupled Silicon strip detectors using pulses from an 1064 nm IR laser, which simulate beam accidents. The voltages on the strips are measured as a function of the bias voltage and compared with the results of DC *I–V* measurements, which are commonly used to characterize the PTP structures. We find that the PTP structures are only effective at very large currents (several mA), and clamp the strips to much larger voltages than assumed from the DC measurements. We also find that the finite resistance of the strip implant compromises the effectiveness of the PTP structures.

Published by Elsevier B.V.

1. Introduction

Silicon strip trackers are an essential component of collider experiments [1]. One concern for their operation is a beam loss, which has been reported to cause sensor damage in the past [2]. A large accumulation of charges in the bulk can collapse the electric field in the sensor, which in turn lets the strip implants float to higher voltages [3]. Since in AC-coupled Silicon strip detectors (SSD) the metal readout traces are held close to ground by the low input impedance of the readout amplifier, very large voltages can develop across the coupling capacitor, which might exceed the specification for its hold-off voltage, which is typically 100 V. If the coupling capacitor is damaged, the AC trace could be shorted to the implant, potentially exposing the readout electronics to large voltages.

In order to prevent these large voltages, the punch-through (reach-through) effect is used [4], which provides over-voltage punch-through protection (PTP) for single strips by shorting strips to the grounded bias line when the strip voltage exceeds a threshold voltage. Although the current ATLAS SCT p-on-n sensors [1] have PTP structures implemented, measurements with a large charge injected with a laser pulse showed that the strips can get damaged [5].

In this paper, we show results from measurement of implant voltages with laser-based charge injection and contrast these dynamic measurements with results from the DC method, which is normally used for PTP structure characterization. This is done on single strips on isolated sensors, without the biasing filtering network used in silicon detector operation, which has been shown to be important [3] and will be part of future studies.

2. Devices

This study investigates several different PTP structures implemented on 1 cm long AC-coupled n-on-p test strip sensors with p-stop isolation made by Hamamatsu Photonics as part of the ATLAS07 sensor run [6] within the ATLAS Upgrade project [7]. Four test sensors (BZ4A–BZ4D) had PTP structures with a channel length to the bias ring of about 20 μm in parallel to the bias resistors, while two test sensors without PTP structures (BZ2 and BZ3) had a channel length of about 70 μm, as had all strip ends opposite to the bias resistors.

3. DC punch-through measurements

The DC method to measure the punch-through effect is described in detail in Ref. [8]. In short, a voltage (V_{test}) is ramped between the strip implant and the grounded bias rail on a detector fully biased to −200 V, and from the measured current i_{test} the (integral) effective resistance R_{eff} (the bias resistance R_{bias} of about

* Corresponding author.
E-mail address: cbetanco1@gmail.com (C. Betancourt).

0168-9002/$ - see front matter Published by Elsevier B.V.
doi:10.1016/j.nima.2011.06.085

Author's personal copy

1.5 MOhm in parallel with the punch-through resistance R_{PT}) is determined. The integral definition for R_{eff} is used in this paper since the integral definition will incorporate the total current than can be drained from the strip to the bias rail, providing the effective resistances through which the charges escape through. The differential resistance used in Ref. [8] is more sensitive to changes in current, and is more useful when analyzing the punch-through voltage V_{PT}.

On ATLAS07 sensors [6] the punch-through voltage V_{PT} is defined as the DC voltage where $R_{eff}=0.5\times R_{bias}$, i.e. $R_{PT}=R_{bias}$. We observed a high degree of uniformity of V_{PT} across the structures with very different channel length: V_{PT} varies only between 20 and 24 V while the channel length varies from 21 μm for BZ4A and BZ4B to ~70 μm for BZ2 and BZ3 [8]. We will see that the effectiveness of PTP structures depends less on V_{PT}, and more on the high current effects where $R_{eff}\sim 1/i_{test}$, which are independent of V_{PT}.

4. Measurements with laser charge injection

4.1. Characteristic of the laser

A more realistic method to study PTP is using ionizing radiation to collapse the electric field in the sensor and then measuring the voltage of the strip implants [3]. As in Ref. [3], the ionizing radiation is provided by a 1064 nm IR "cutting" laser, Alessi LY1. The laser sends out pulses of less than 1 μs width with ~4 μs separation. Every laser pulse creates a large amount of charge (~3×10^{7} MIPs, or about 1 Rad per pulse) in the Si sensor and the intensity can be reduced with a filter wheel. The amount of charge deposited per pulse was determined by integrating the signal on the AC pad, which was terminated with a 50 Ω resistor. The amount of deposited change can be increased by increasing the number of laser pulses. Voltage saturation of the DC signal is seen after one laser pulse, indicating complete field breakdown, with subsequent pulses showing decreased amplitude.

4.2. Characteristic of the voltage transients on the implants

The sensors were biased to −200 V, unless scanned, and the power supply currents were recorded, but not used in the PTP evaluation. The voltages on the DC pads located at both end of a strip are readout through high impedance voltage dividers into a digital scope, which preserves the < 1 μs rise time, as can be seen by the shapes of the recorded voltage transient shown in Fig. 1. We find that the peak voltages of the transients occur at about 1 μs after firing of the laser and are independent of the laser power, i.e. the number of laser pulses. This can be explained by the fact that the first laser pulse decreases the sensitivity of the sensor sufficiently such that following pulses do not cause further large voltage increases.

The laser focal spot size is 10 um, yet a scan of neighboring strips shown in Fig. 2 reveals elevated voltages on the neighboring strips, indicating the size of the breakdown region is of the order ~1 mm or more. As already shown in Fig. 1, increasing the laser intensity by increasing the number of pulses from one to three does not increase the peak voltage next to the laser pulse, but Fig. 2 shows that this raises the potential in the neighboring strips, indicating that the breakdown at a distance from the laser is not complete. The Al readout strip above the implant being tested is held to ground via a 50 Ω impedance, but Fig. 2 shows that whether the AC strip is grounded or floating did not affect the peak voltage close to the laser spot. Our measurements were done with one laser pulse and the AC strip floating, unless stated otherwise.

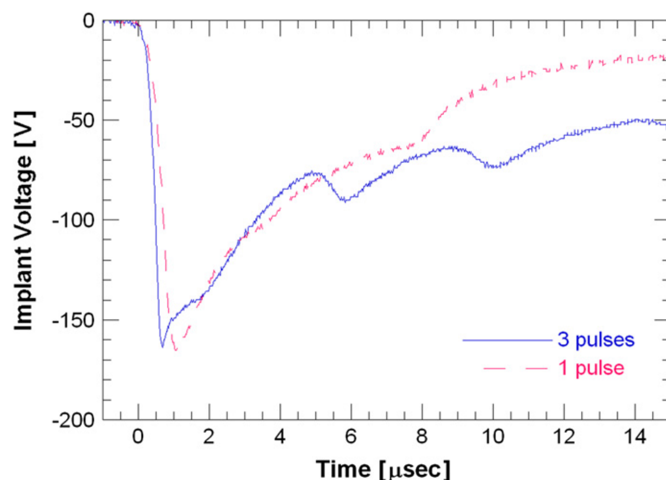

Fig. 1. Voltage transients on the implant next to the IR laser spot of test sensor W51-BZ4D biased at 200 V for two laser intensities, one pulse and three pulses, respectively. The laser is focused at the "far end" and the voltage, V_{far}, is measured there (see Fig. 5).

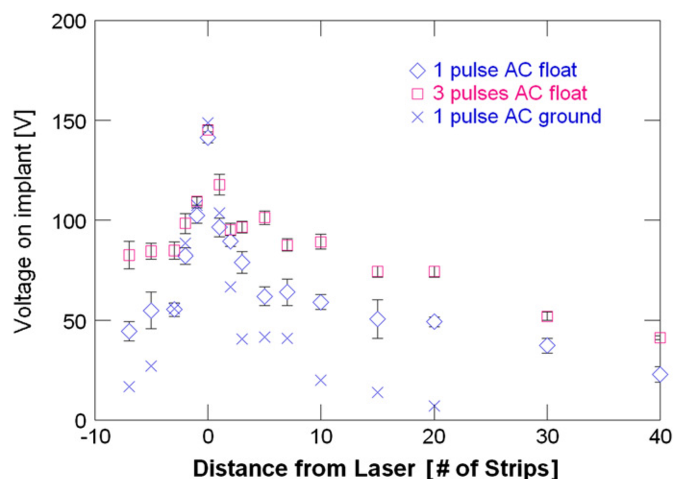

Fig. 2. Implant peak voltage as a function of the distance from the laser spot in number of strips of 74.5 μm pitch on W51-BZ4C biased at 200 V. The peak voltages are measured for two laser intensities, one pulse and three pulses, respectively, and also for grounded and floating AC trace.

4.3. Punch-through indicated by voltage transients

The strip peak voltage of about 150 V in Figs. 1 and 2 is a large fraction of the bias voltage, indicating that the field in the sensors is indeed collapsed and that the PTP structure is not effective in this case, where the laser is located at the "far end" and the voltage "V_{far}" is measured there (see Fig. 5 below). The effectiveness of the PTP is shown in Fig. 3 by plotting the voltage on the DC pad next to the PTP structure ("V_{near}") for the cases where the laser is positioned either next to the PTP structure ("Laser near") or on the opposite strip end ("Laser far"). Now the PTP structures BZ4A–BZ4C clamp the voltage at finite voltages of about 69–100 V (highlighted by the horizontal lines), independent of the bias voltage and the laser position, albeit at much larger voltages than the DC V_{PT}, which is indicated as a band in Fig. 3. In contrast, the test sensors without PTP structure (BZ2 and BZ2) do not show saturation and their voltages keep rising with the bias voltage. All measurements are done with AC strips floating.

The observations that the implant voltages of the different structures show such large differences even though the DC

Author's personal copy

Fig. 3. Peak voltages V_{near} measured at the "near" implant location as a function of the bias voltage. The data with laser "near" injection are shown with filled symbols and the letter "N". The data with laser "far" location are shown with open symbols and the letter "F". The DC PT voltages, as defined in Section 3, are shown as a band.

punch-through voltages are so similar, and why the voltages depend so strongly on the location with respect to the punch-through structure will be briefly explained in the following sections and fully explained in a follow up paper.

5. DC voltage and current dependence of the punch-through resistor

The fairly high voltages observed in Figs. 1–3 indicate that when the field collapses, the PTP structures do not clamp the strips to ground, but still have a finite resistance. This means that the voltage dependence of the PTP resistance R_{PT} (V) has to be examined to find the voltage when R_{PT} reaches a sufficiently small value, and that is certainly not the punch-through voltage V_{PT}, which for ATLAS07 sensors was defined by R_{PT} (V_{PT})$=R_{bias}$, i.e. very far from a "short" to the bias line.

When extending the DC I–V curves to voltages much larger than V_{PT}, the punch-through resistance continues to decrease, as seen in Fig. 4a. The voltages at which the different structures reach values of the order 10 kΩ are now very different from each other. As discussed later in Section 6, this will explain the difference in voltages exhibited in Fig. 3 of different PTP structures. Remarkably, as shown in Fig. 4b, all structures show very similar resistance vs. current ($R_{eff}-i_{test}$) dependence, with 10 kΩ reached at fairly high currents of about 10 mA. Thus the punch-through protection will depend on the voltage at which such currents can be delivered through the PTP structure. Note that the observed current dependence $R_{PT}\sim 1/i_{PT}$ is predicted for PTP structures in Refs. [9,10] for large currents.

6. The 4-resistor model for the laser measurements

Implant voltages were taken at the peak value of the transients, i.e. when $dV/dt=0$, which means that we are dealing with a quasi-DC problem with essentially ohmic, but dynamic resistors. The very different implant voltages for the same PTP structures but different laser locations shown in Figs. 2 and 3 emphasize the need to account for all resistors in the system. In order to predict and understand the effectiveness of different PTP structures during beam accidents, one needs to calculate the voltages and

Fig. 4. DC scan of effective resistance R_{eff} as a function of (a) applied voltage and (b) current, between strip DC pad and the bias ring, respectively. One probe is used to stimulate and measure. The resistance–voltage scan is an extension to higher voltages of the data of Ref. [8], where $V_{PT}\approx 20$ V was found.

Fig. 5. Schematic of the "4-R" resistor network in laser injection measurements. The suffix "near" indicates the DC pad closest to the bias resistor, "far" indicates the DC pad at the opposite end of the strip.

currents correctly. We argue that a simple "Four Resistor (4-R) Model" can do this (Fig. 5). It consists of the following four resistances: R(near)$=R_{eff}$ ($\approx R_{PT}$(near) at high currents, where R_{PT}(near) is the PT resistor next to the bias resistor

Author's personal copy

$R_{bias} \approx 1.5$ MΩ), R_{PT}(far)=resistance on the far end of the strip (opposite to the bias resistance), R_{imp}=resistance of the implant, measured to be 15 kΩ/cm, and finally R_b=resistance of the bulk.

All resistors besides the measured R_{imp} and R_{bias} can be determined from the laser data, because the laser is fired alternatively near and far and the voltages both near (V_{near}) and far (V_{far}) are measured simultaneously. The voltage drop across R_{imp} permits the determination of all the currents in the resistor network Fig. 5. The near side punch-through current i_{PT}(near) is calculated by

$$i_{PT}(\text{near}) = \frac{V_{far} - V_{near}}{R_{imp}}$$

and is measured when the laser is at the far end. The far side punch-through current i_{PT}(far) is given by

$$i_{PT}(\text{far}) = \frac{V_{near} - V_{far}}{R_{imp}}$$

and is measured when the laser is at the near end. Given the different channel lengths of the PTP structures mentioned above, we expect that $R_{PT}(\text{far}) > R_{PT}(\text{near})$ for the PTP structures, and $R_{PT}(\text{far}) \approx R_{PT}(\text{near})$ for BZ3 and BZ2, which do not have PTP structures.

6.1. Bulk resistance

The current dependence of the bulk resistance R_b, shown in Fig. 6 for the laser in both positions. The bulk resistance for the laser far measurements is $R_b = (V_{bias} - V_{far})/i_b$ and for the laser near measurements is $R_b = (V_{bias} - V_{near})/i_b$, where i_b is the bulk current and is the sum of i_{PT}(near) and i_{PT}(far). The bulk resistance is shown in Fig. 6 for the laser in both positions and is independent of the current through the bulk and about the same for both laser positions.

The value of the bulk resistance can also explain the different implant voltages measured for different PTP structures. Neglecting punch-through on the far side, we can write the near side implant voltage as

$$V_{near} = \frac{R_{eff}}{R_{eff} + R_b} V_{bias}$$

So that implant voltage is determined by the interplay between the effective resistance (punch-though and bias resistor) and the bulk resistance. Since different PTP structures have different R_{eff} from each other, we expect the voltages differ among different PTP structures.

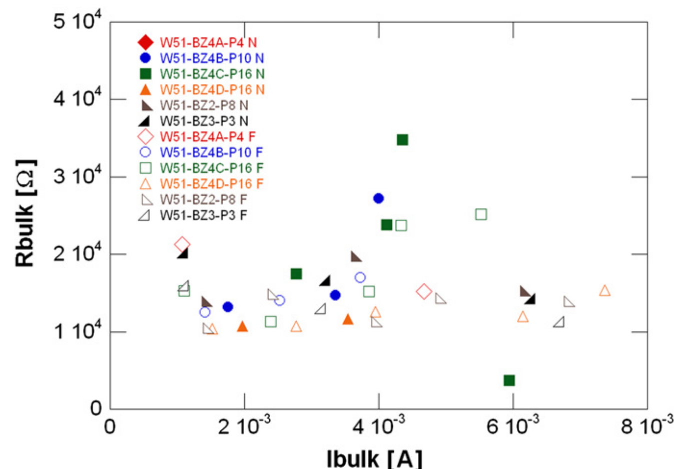

Fig. 6. Current dependence of the bulk resistance R_{bulk} for both laser positions.

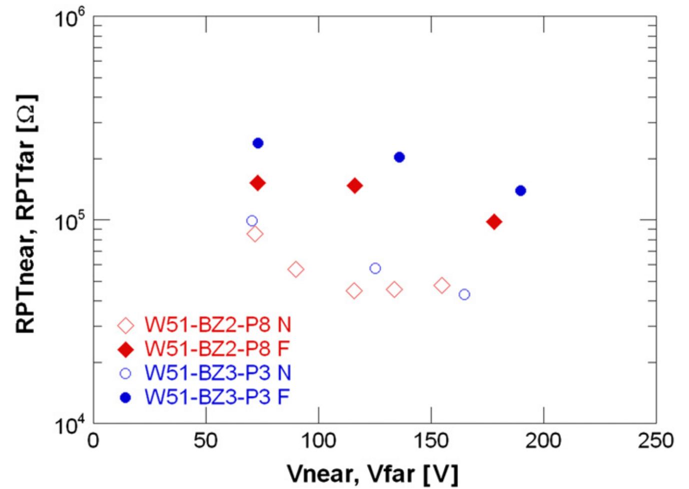

Fig. 7. Voltage dependence of the resistance R_{PT} for the structures BZ2 and BZ3 without PTP structure. Open symbols are R_{PT}(near), filled symbols are R_{PT}(far).

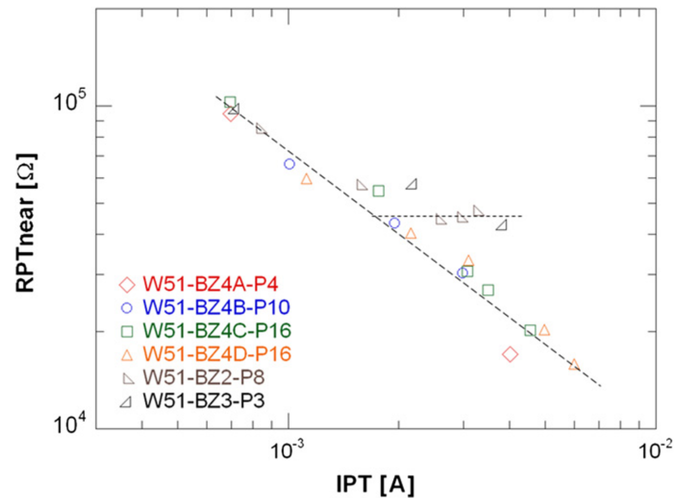

Fig. 8. Current dependence of R_{PT}(near) showing the approximate $1/i$ dependence and the leveling-off of the non-PTP structures BZ2 and BZ3. The lines are to guide the eye.

6.2. Gate effect of bias resistor

We note the influences of the bias resistor on the resistance of the channel of R_{PT}(near). Fig. 7 shows that for the structures BZ2 and BZ3 without PTP structure, the resistance close to the bias resistance R_{PT}(near) is significantly lower than the resistance at the opposite end R_{PT}(far). We can attribute this fact to the presence of the polysilicon bias resistor close to the "near" DC pad, acting as a gate. In addition, we observe in Figs. 3 and 4, that of the PTP structures, BZ4A shows smaller saturation voltage and smaller R_{PT} than the other PTP structures, which can be explained by the fact that the trace of the bias resistance crosses the channel in an optimal location for BZ4A, while it is peripheral to the channel for the other test structures.

6.3. Punch-through and space-charge limited (SCL) regions

Following Refs. [9,10] there are two different regions in I–V characteristics of PTP structures: an exponential current rise in the punch-through region, and a space-charge limited (SCL) region at higher voltages. In the punch-through region, the punch-through resistance varies approximately inversely with the current, which is shown in Fig. 8. This leads to a saturation

Author's personal copy

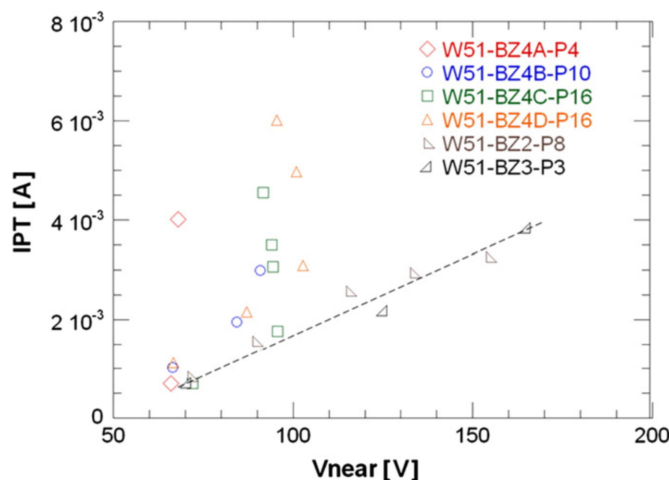

Fig. 9. Voltage dependence of the current in the PTP channel. The line connecting the non-PTP structures BZ2 and BZ3 suggest a linear dependence, while the PTP structures show a much more rapid rise of the current with the voltage.

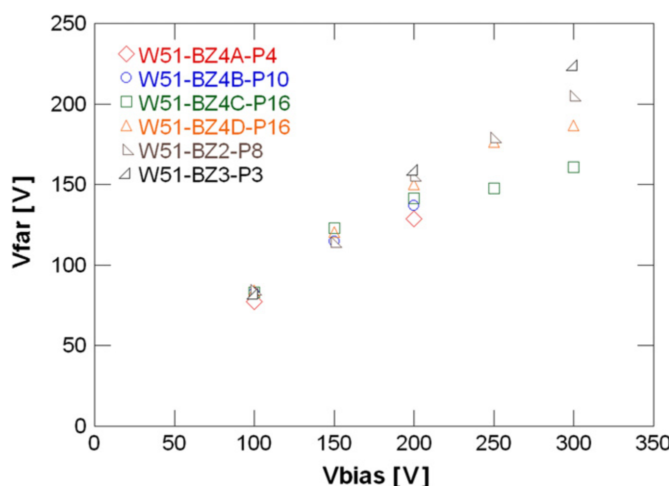

Fig. 10. Voltages V_{far} measured at the "far" implant location as a function of bias voltage. The laser pulse was injected at the "far" location as well. This should be compared with Fig. 3, where V_{near} showed saturation for the PTP structures below or at about 100 V.

of the voltage $V \sim i_{PT} \times R_{PT}$ seen in Fig. 3. In the SCL region, the resistance is predicted to saturate to a finite value, which only depends on the geometry of the structure and bulk properties of the silicon [9,10]. This trend is seen in Fig. 8 for the structures without PTP, BZ2 and BZ3.

Different voltage dependences of the current (I–V) are predicted for the punch-through and SCL region, respectively: in the punch-through region, the current increases exponentially with the voltage, while in the SCL region the current depends linearly on the voltage. In the I–V plots of Fig. 9, all structures with PTP (i.e. BZ4A–BZ4D) appear to be in the punch-through region, while the non-PTP structures (BZ2 and BZ3) show an I–V dependence consistent with SCL as indicated by the straight line.

6.4. *Effect of the finite implant resistance*

The finite resistance of the strip implant plays a pivotal role in isolating the strip voltages from the PTP structures if the breakdown occurs at the far end ("Laser Far"). In Fig. 10, the V_{far} voltage shows no saturation even for detectors with the PTP structures. This is very different from the saturation of V_{near} for several sensors with the PTP structures shown in Fig. 3. The difference between the V_{far} and V_{near} is $R_{imp} \times i_{PT}$, and since i_{PT} is of the order a 5–10 mA at punch-through, and $R_{imp} \approx 15$ kΩ, the voltage difference between V_{far} and the saturated V_{near} can reach 100s of volt.

7. Conclusions

We have used an IR cutting laser to simulate a beam accident in silicon sensors: a large amount of charge is created in the bulk, the E-field collapses and the implants can float to a large voltage. This allows us to test the effectiveness of punch-through protection structures implemented on n-on-p test sensors to prevent large voltages on the implants.

Our measurements indicate that the dynamic scenario of large injected charge is not accurately characterized by the traditional DC measurements. In all cases, the voltages recorded on the implants when the field collapses are much higher than the corresponding DC punch-through voltage. The explanation for this effect is a non-zero resistance of the punch-through structure, which, depending on the current through the structure and the structure type, can be much larger than other resistances in the system, e.g. the implant resistance and the bulk silicon resistance after the field collapse.

The observed dependence of R_{PT} on the inverse of the current is explained by the theory. For sensors with dedicated PTP structures, the voltages observed on the DC pad closest to the bias resistance (where PTP structures are implemented) saturate as a function of bias voltage due to large currents flowing through R_{PT}. Although the voltages are fairly large, this holds a promise for constraining implant voltages with more optimized structures, including the reduction of the channel length and the use of gates.

The voltages measured at the "far" end of the strip do not show saturation, since the finite resistance of the strip implant effectively isolates that region from the PTP structure. This indicates the need for lowering the resistivity of the strip implants, since the current needed to activate the PTP is of the order of mA, at which point their resistance is reduced to sufficiently low values.

Future work will focus on testing structures with different p-spray and p-stop implantation doses, the effect of sensors having different channel lengths, testing irradiated sensors, and investigating the effect of the backplane RC bypass filter on the high implant voltages.

References

[1] Y. Unno, et al., Nucl. Instr. and Meth. A 511 (2003) 58.
[2] A. Litke, Private Communication.
[3] T. Dubbs, M. Harms, H.F.-W. Sadrozinski, A. Seiden, M. Wilson, IEEE Trans. Nucl. Sci. NS-47-6 (2000) 1902.
[4] J. Ellison, et al., IEEE Trans. Nucl. Sci. NS-36-1 (1989) 267.
[5] K. Hara, et al., Nucl. Instr. and Meth. A 541 (2005) 15.
[6] Y. Nobu, et al., Nucl. Instr. and Meth. A (2010). doi:10.1016/j.nima.2010.04.080.
[7] I. Dawson, The ATLAS Tracker Upgrade, This Conference.
[8] S. Lindgren, et al., Nucl. Instr. and Meth. A (2010). doi:10.1016/j.nima.2010.04.094.
[9] J.I. Chu, G. Persky, S.M. Sze, J. Appl. Phys. 43 (1972) 3510.
[10] J. Lohstroh, et al., Solid-State Electron. 24 (1981) 805.